Available online at www.sciencedirect.com
SCIENCE DIRECT
ELSEVIER
Polymer 46 (2005) 2506–2521
polymer
www.elsevier.com/locate/polymer

Investigation of ionomers as dispersants for single wall carbon nanotubes

D.M. Delozier*[1], D.M. Tigelaar[1,2], K.A. Watson[3], J.G. Smith Jr., D.J. Klein[3], P.T. Lillehei, J.W. Connell

NASA Langley Research Center, Advanced Materials and Processing Branch, Hampton, VA 23681-2199, USA

Received 16 July 2004; received in revised form 18 January 2005; accepted 19 January 2005

Abstract

A novel conjugated ionomer was prepared from a diamine and a bis(pyrylium salt). Single-walled carbon nanotubes (SWNT) were dispersed in solutions of the ionomer in *N*,*N*-dimethylacetamide resulting in homogenous suspensions or quasi-solutions. These suspensions were used to cast unoriented thin films. In addition, the ionomer/SWNT solutions were used to aid in the dispersal of SWNTs in a soluble, low color polyimide. The use of the ionomer as a dispersant enabled the nanotubes to be dispersed at loading levels up to 1 wt% in a polyimide solution without visual agglomeration. SWNTs were well dispersed in the thin films as evidenced by visual inspection, optical microscopy, and high resolution scanning electron microscopy. The films were further characterized for their electrical and mechanical properties.
© 2005 Elsevier Ltd. All rights reserved.

Keywords: Polyimides; Poly(pyrylium salts); Modified nanotubes

1. Introduction

Potential applications for single wall carbon nanotube (SWNT) containing materials are numerous; however, full implementation of technology involving SWNTs will not be realized until issues involving SWNT purity and dispersion are resolved. The dispersion of SWNTs into polymers has been difficult due to many factors, including the inability to interface with polymers and the inherent bundling of the tubes due to the strong van der Waal forces present between tube surfaces [1]. Even in highly aromatic polyimides, the maximum loading level that is attainable while maintaining good dispersion is approximately 0.2 wt% [2–5]. Additionally, the shape of the tubes aids in the bundling effect as the long rope-like structures intertwine, creating vast networks of tightly bound tubes. Although some mechanical methods such as sonication [5] and homogenization [6] have been successfully employed for dispersing SWNTs networks, the networks are not easily separated into small bundles because of their small dimensions.

Other methods which involve non-mechanical schemes have also been employed to disperse SWNTs. One dispersal method involves the attachment of various functional groups to the side walls and ends of the SWNTs. These groups act both as handles for further reaction as well as to create separation between the tube surfaces [7–15]. These covalent modifications work well in some instances for dispersing SWNTs in organic solvents, but in order for this method to be useful for dispersing SWNTs in polymers the extent the surface has to be modified significantly alters the mechanical and electrical properties of the SWNTs. An alternate approach for improving SWNT dispersion in polymers consisted of having reactive groups on the polymer that react with functionality present on the nanotube surface resulting from purification [16].

Non-covalent modifications to the SWNTs are also being used for dispersing SWNTs and appear to be the best way to disperse the nanotubes without adversely affecting the properties of the nanotubes. A method of dispersing SWNTs has employed the use of surfactants, allowing high concentrations (20 mg/ml) of SWNTs to be dispersed in

* Corresponding author. Tel.: +1 757 864 4268; fax: +1 757 864 8312.
E-mail address: d.m.delozier@larc.nasa.gov (D.M. Delozier).
[1] National Research Council.
[2] NASA Glenn Research Center, 21000 Brookpark Rd., Cleveland, OH 44135, USA.
[3] National Institute of Aerospace, 144 Research Drive, Hampton, VA 23666, USA.

0032-3861/$ - see front matter © 2005 Elsevier Ltd. All rights reserved.
doi:10.1016/j.polymer.2005.01.051

aqueous media [17]. However, surfactants typically do not function well in organic solvents thus preventing effective dispersion of high weight fractions of SWNTs in polymers. Similar modifications have been performed in organic solvents where the van der Waal attractions that some polymers and small molecules have for the nanotube surfaces are utilized. The attraction that these molecules have for the nanotube surfaces causes them to align along the tube surface or wrap the tube, thus increasing its solubility [18–20]. The use of this type of non-covalent modification to disperse SWNTs usually involves π-conjugated small molecules or polymers [21–30]. Conjugated polymers such as poly(*m*-phenylenevinylene) (PmPV) [31] and poly(phenylacetylene) [32] disperse SWNTs in organic solvents. Coulombic attraction of molecules to the nanotube surface has also aided in nanotube dispersion as ionic polymers [33,34] and ionic liquids [35] have been shown to disperse SWNTs in organic solvents.

In the work described herein a polymer was developed that possesses those features described above as non-covalent modification. An aromatic, conjugated ionomer with alkyl side chains was chosen to disperse large weight fractions of SWNTs. Based on the chemical structure, the ionomer was expected to have favorable van der Waal and Coloumbic interactions with the nanotube surface. Thin films were prepared from ionomer/SWNT solutions and ionomer/SWNT/polyimide solutions. This was done to determine the effect of the addition of SWNTs on the properties of the ionomer as well as the polyimide. This approach allowed for improved dispersions of SWNTs of higher weight loadings in the polyimide than was achievable without the use of the ionomer as a dispersing aid. Once thermally dried, the films were characterized for physical, mechanical and electrical properties. The chemistry and properties of these materials and resultant nanocomposites are discussed.

2. Experimental

2.1. Starting materials

Bucky Pearl SWNTs (90% purity) were purchased from Carbon Nanotechnologies Incorporated (Houston, TX 77084) and treated as described in Section 2.3. 1,3-Bis(3-aminophenoxy)benzene [APB, Mitsui Chemicals America, Inc. melting point (mp) 107–108.5 °C] was used as received. 4,4′-Hexafluoroisopropylidiene dipthalic anhydride (6-FDA, Hoechst Celanese Inc., mp 241–243 °C) was sublimed prior to use. High molecular weight LaRC™ CP2 was purchased from SRS Technologies, Inc. (Huntsville, AL 35806) and used as received. *N*,*N*-Dimethylacetamide (DMAc), dimethyl sulfoxide (DMSO), pyridine, methanol, sodium methoxide (NaOMe), and 1,2-dichlorobenzene (ODCB) were received in reagent grade from Aldrich Chemical Company and used as received. 9,9-Dioctylfluorene was prepared according to a literature procedure [36]. All other materials were purchased from commercial sources and used without further purification.

2.2. Preparation of monomers used in ionomer synthesis

2.2.1. 2,7-Dinitro-9,9-dioctylfluorene

Into a 1 l, three-necked flask equipped with a mechanical stirrer and an addition funnel were charged 9,9-dioctylfluorene (30.53 g, 26.56 mmol) and glacial acetic acid (150 ml). The biphasic mixture was stirred while cooling to 0 °C by submersing the flask into an ice bath. Fuming nitric acid (150 ml) was added dropwise through the addition funnel over 45 min. The bath was slowly warmed to 55 °C over a period of 2 h and subsequently turned off. The reaction was allowed to continue at room temperature overnight, during which time a tacky, orange precipitate formed. The contents of the reaction were slowly poured into 1.2 l ice water and stirred for 1 h. The water was decanted from the solid and the product washed several times with water. The product was dissolved in 400 ml chloroform ($CHCl_3$) and washed sequentially with 200 ml each of water, brine, and water. The organic layer was collected, dried over magnesium sulfate and filtered. The filtrate was evaporated to dryness to afford a viscous orange liquid. This liquid was dissolved in 200 ml hexanes and precipitated by submersing the flask in a dry ice/acetone bath. A yellow solid was collected via filtration and washed with cold hexanes. The product was dried at room temperature and used without further purification (mp 69–73 °C). Yield = 27.84 g (75%). ^{1}H NMR ($CDCl_3$) δ 0.5 (m, 4H), 0.8 (t, 6H), 1.0–1.3 (m, 20H), 2.1 (m, 4H), 7.9 (s, 1H), 8.0 (s, 1H), 8.3 (d, 2H), 8.3 (d, 1H), 8.3 (d, 1H) ppm. ^{13}C NMR ($CDCl_3$) δ 14, 23, 24, 29, 29, 29, 30, 32, 40, 57, 119, 122, 124, 145, 149, 154 ppm. IR (KBr) υ (cm^{-1}) 3086, 3074 (Ar–H), 2953, 2919, 2852 (alkyl-H), 1588 (Ar), 1521, 1341 (–NO_2). Elemental analysis calculated for $C_{29}H_{42}N_2O_4$: %C, 72.47; %H, 8.39; %N, 5.83; Found: %C, 72.12; %H, 8.02; %N, 6.02.

2.2.2. 2,7-Diamino-9,9-dioctylfluorene (AFDA)

2,7-Dinitro-9,9-dioctylfluorene (27.84 g, 57.93 mmol) was dissolved in absolute ethanol (90 ml) and tetrahydrofuran (THF, 50 ml) in a 300 ml Parr bottle. Palladium on carbon (5%, 0.5 g) was subsequently added and the mixture was placed on a Parr hydrogenator and shaken under 40 psi of hydrogen for 4 h at room temperature. The mixture was filtered through Celite® and the solvent removed by rotary evaporation to afford a viscous red–brown liquid. The crude product was dissolved in $CHCl_3$ and stirred with decolorizing charcoal for 1 h at room temperature. The solution was filtered and the solvent removed by rotary evaporation to give a red oil that slowly solidified into needle-like crystals (mp 58–63 °C). Yield = 22.36 g (92%). ^{1}H NMR ($CDCl_3$) δ 0.7 (m, 4H), 0.8 (t, 6H), 1.0–1.3 (m, 20H), 1.9 (m, 4H), 3.6

(s, 4H), 6.6 (m, 4H), 7.3 (d, 2H) ppm. ^{13}C NMR ($CDCl_3$) δ 15, 23, 24, 30, 30, 31, 32, 41, 55, 111, 114, 119, 134, 145, 152 ppm. IR (KBr) υ (cm^{-1}) 3447, 3408, 3356, 3329 (–NH_2), 3003 (Ar–H), 2956, 2926, 2853 (alkyl-H), 1617 (Ar). Elemental analysis calculated for $C_{29}H_{46}N_2$: %C, 82.80; %H, 10.54; %N, 6.66; Found: %C, 82.29; %H, 10.06; %N, 6.73.

2.2.3. 3,3′-(1,4-Phenylene)bis(1,5-di(4-fluorophenyl))-1,5-pentadione

Into a 1 l, three-necked flask equipped with a mechanical stirrer and an addition funnel were charged terephthalaldehyde (13.40 g, 99.87 mmol) and 95% ethanol (550 ml). 4-Fluoroacetophenone (77.61 g, 588.9 mmol) was added and the suspension was heated while stirring until all of the terephthalaldehyde dissolved. A solution of potassium hydroxide (8.42 g, 150 mmol) in water (60 ml) was subsequently added dropwise through the addition funnel over 30 min. A lemon-yellow precipitate of the bis-chalcone formed almost immediately. The reaction mixture was heated to reflux for 30 h, during which time the solid slowly dissolved. The reaction mixture was slowly cooled to room temperature to afford a yellow precipitate. The solid was collected by vacuum filtration, washed with cold ethanol, and dried under vacuum at 100 °C for 3 h. The pale yellow product was used without further purification (mp 144–157 °C). Yield = 58.27 g (90%). ^{1}H NMR ($CDCl_3$) δ 3.1–3.5 (m, 8H), 4.1 (m, 2H), 7.1 (t, 8H), 7.2 (s, 4H), 7.9 (t, 8H) ppm. ^{13}C NMR ($CDCl_3$) δ 37, 45, 114, 116, 128, 131, 133, 142, 165, 197 ppm. IR (KBr) υ (cm^{-1}) 3073 (Ar–H), 2982, 2904 (alkyl-H), 1685 (C=O), 1598,1506 (Ar), 1231 (Ar–F). Elemental analysis calculated for $C_{40}H_{30}F_4O_4$: %C, 73.84; %H, 4.65; %F, 11.68; Found: %C, 73.56; %H, 5.03; %F, 11.11.

2.2.4. 1,4-Bis(4-(2,6-di(4-fluorophenyl)pyrylium))benzene ditriflate (BPBD)

Into a 500 ml, three-necked flask equipped with a mechanical stirrer and an addition funnel was charged triphenylmethanol (23.73 g, 91.15 mmol) and acetic anhydride (150 ml). The reaction flask was cooled to 0 °C in an ice bath and 50% trifluoromethylsulfonic acid (34.53 g, 115.0 mmol) was added over 30 min through the addition funnel. One hour after the addition was complete, finely ground 3,3′-(1,4-phenylene)bis(1,5-di(4-fluorophenyl)-1,5-pentadione (24.34 g, 37.41 mmol) was added. The ice bath was subsequently removed and the reaction mixture stirred overnight at room temperature. A bright red solid was collected by vacuum filtration, washed with ether, and dried under vacuum for 2 days at 100 °C (dec 355 °C). Yield = 22.67 g (67%) ^{1}H NMR (DMSO-d_6) δ 7.5–7.9 (m, 8H), 7.9–8.3 (m, 4H), 8.3–8.7 (m, 8H), 9.0 (s, 4H) ppm. IR (KBr) υ (cm^{-1}) 3074 (Ar–H), 1616, 1501 (Ar), 1253 (Ar–F). Elemental analysis calculated for $C_{42}H_{25}F_9O_8S_2$: %C, 55.39, %H, 2.66; %F, 20.86; Found: %C, 55.59; %H, 2.62; %F, 20.47.

2.3. Preparation of soluble nanotubes (s-tubes)

Into a 250 ml, round bottom flask were placed 0.3 g of SWNT and 660 ml ODCB. The flask was placed in a Branson 2510 Bransonic® ultrasonic cleaner bath operating at 42 KHz for 3 h. In a separate flask were placed 0.792 g NaOMe and 240 ml pyridine. This mixture was stirred with a magnetic stirbar. The nanotube suspension was subsequently added to the pyridine/NaOMe solution. The mixture was heated to 80 °C while stirring under a nitrogen atmosphere for 16 h followed by 3 h at reflux (~150 °C). Pyridine was removed by distillation, followed by collection of the nanotubes via centrifugation. The nanotubes were washed three times with methanol via suspension and centrifugation. The nanotubes were then dried under vacuum for 24 h at room temperature resulting in a black powder [yield = 0.451 g] [37].

2.4. Preparation of ionomer for use as a dispersant (d-ionomer)

Into a 500 ml, three-necked flask equipped with nitrogen inlet, mechanical stirrer, and drying tube were placed AFDA (5.88 g, 14.0 mmol) and DMSO (90 ml). The reaction mixture was stirred until the diamine completely dissolved. BPBD (12.82 g, 14.0 mmol) was added as a powder followed by additional DMSO (90 ml). While stirring, the flask was slowly heated to 165 °C in an oil bath and held for 5 h. DMSO (90 ml) was added to the solution and upon cooling to room temperature the solution was subsequently poured into water (2 l) while in a Waring blender. The resulting fibers were washed with warm water and then dried under vacuum at 100 °C for 24 h. [inherent viscosity(η_{inh}) = 1.95 dl/g].

2.5. Preparation of ionomer-nanotube (IN) films

Into a 100 ml, three-necked flask equipped with nitrogen inlet, mechanical stirrer, and drying tube were placed s-tubes (21.1 mg) and DMAc (40 ml). The flask was placed in a Branson 2510 Bransonic® ultrasonic cleaner bath operating at 42 KHz for 1 h followed by the addition of d-ionomer (200 mg). This suspension was sonicated for an additional 0.5 h. AFDA (0.6033 g, 1.43 mmol) was subsequently added and sonication continued for 1 h. BPBD (1.3042 g, 1.43 mmol) was added and the reaction mixture stirred and sonicated until the pyrylium salt was well dispersed (~1 h). The flask was subsequently immersed in an oil bath. A Dean-Stark trap was added in place of the drying tube and the reaction mixture was slowly heated to 165 °C. DMAc and the water of reaction were removed from the reaction via the Dean-Stark trap. The amount of DMAc that was collected into the trap was measured. The solvent was replenished as cool DMAc (25 °C) was slowly added to the reaction flask at various times during the reaction. The reaction was stopped after 3 h at 165 °C and the polymer

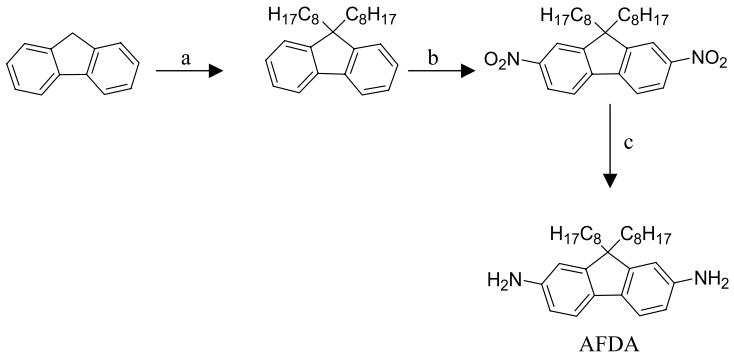

Fig. 1. Synthetic route to AFDA (a) THF, *n*-BuLi, *n*-octyl bromide, −78 °C (b) acetic acid, fuming nitric acid, 55 °C (c) 5% Pd/C, hydrogen (40 psi), THF/EtOH.

solution was poured into water (1 l) in a blender, resulting in greenish-black fibers. The fibers were subsequently washed with warm water and dried in a forced air oven at 125 °C for 2 h. The fibers (0.69 g) were then dissolved in DMAc (5 ml) and stirred while sonicating for 2 h. A film was cast from this solution.

Control films containing no nanotubes were prepared in the same way from the ionomer (η_{inh} of 1.24 dl/g).

2.6. Preparation of polyimide-ionomer-nanotube (PIN) nanocomposites via simple mixing

Into a 25 ml, round bottom flask equipped with a ground glass stopper were placed s-tubes (8.5 mg) and DMAc (3.02 g). The flask was placed in a Branson 2510 Bransonic® ultrasonic cleaner bath operating at 42 KHz for 1 h followed by the addition of d-ionomer (0.2556 g) and DMAc (2.26 g). The suspension was sonicated for an additional hour to give a homogeneous suspension. Into a separate 50 ml, three-necked flask equipped with nitrogen inlet and a mechanical stirrer were placed LaRC™ CP2 polyimide (0.85 g) and DMAc (1.5422 g). The solution was stirred for 1 h at room temperature, and the ionomer-nanotube solution was added dropwise to the LaRC™ CP2 solution while stirring and sonicating. DMAc (2.2 g) was used to wash in the remaining ionomer-nanotube solution, and the entire contents were stirred for 1 h and subsequently used to cast a film.

2.7. Preparation of polyimide-ionomer-nanotube nanocomposites via in-situ polymerization (IS-PIN)

Into a 100 ml, three-necked flask equipped with nitrogen inlet, mechanical stirrer, and drying tube were placed s-tubes (20 mg) and DMAc (9 ml). The s-tubes were sonicated in a Branson 2510 Bransonic® ultrasonic cleaner bath operating at 42 KHz for 2 h followed by the addition of d-ionomer (50 mg). Sonication continued for 1 h followed by the addition of APB (0.7933 g, 2.71 mmol) as a powder. The reaction mixture was stirred and sonicated for an additional hour followed by the addition of 6-FDA (1.2051 g, 2.71 mmol) as a powder. DMAc was used to wash the sides of the flask and the reaction was stirred under sonication for an additional 1 h. Sonication was stopped and the polymer solution stirred for 16 h at room temperature.

This procedure was repeated with as-received (neat tubes) SWNTs.

2.8. Thin films

Thin films were cast from control solutions and nanocomposite mixtures from DMAc. The neat solutions and the IS-PIN mixtures were doctored onto plate glass and dried to a tack-free state under flowing air at room temperature in a low humidity chamber. All other s-tube containing films were cast on glass that had been warmed to 60 °C and were heated at this temperature in flowing air until tack free. To effect solvent removal the thermal conditions in flowing air after drying to a tack-free film were 1 h each at 100, 150, and 220 °C. The in-situ PIN nanocomposites required an additional hour at 300 °C to effect imidization. Thin-film tensile properties were determined in the direction transverse to the draw direction as recommended in ASTM D882 at room temperature using five specimens from each film at a rate of 0.5 mm/min.

2.9. Characterization

Elemental analyses were performed by Desert Analytics (Tuscon, Arizona). High resolution scanning electron microscopy (HRSEM) images were obtained on a Hitachi S-5200 field emission scanning electron microscopy system operating at or below 5.0 kV. Optical microscopy was performed using an Olympus BH-2 at a magnification of 50×. Surface resistivity was determined according to ASTM D-257-99 using a Prostat® PSI-870 surface resistance and resistivity indicator operating at 9 V, and reported as an average of three readings. Volume resistivity was determined using a Prostat® PRS-801 Resistance System with a PRF-911 Concentric Ring Fixture operating at 10–100 V according to ASTM D-257. Melting point ranges (tangent of onset to melt and the endothermic peak) were

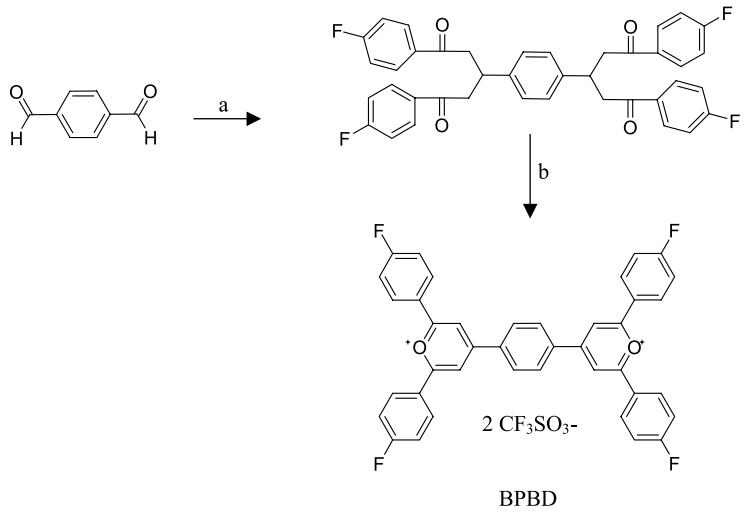

Fig. 2. Synthetic route to BPBD (a) 95% ethanol, 4-fluoroacetophenone, KOH/H_2O, reflux (b) acetic anhydride, triphenylmethanol, 50% trifluoromethylsulfonic acid.

determined by differential scanning calorimetry (DSC) at a heating rate of 10 °C/min. Raman spectroscopy was performed using a Thermo Nicolet Almega Dispersive Raman spectrometer equipped with a 785 nm laser. ^{1}H NMR spectra were obtained on a Bruker Avance 300 MHz spectrometer at 300 MHz with TMS as an internal standard. ^{13}C NMR were obtained at 75 MHz. Inherent viscosities were obtained for 0.5% (w/v) solutions in DMAc at 25 °C. Fourier Transform Infrared (FTIR) spectra were obtained on a Nicolet Magna-IR™ 750 spectrometer. Ultraviolet/visible/near infrared (UV/Vis/NIR) spectra were obtained on thin films using a Perkin–Elmer Lambda 900.

3. Results and discussion

3.1. Preparation of monomers and ionomer

The diamine and the pyrylium salt monomers were prepared as shown in Figs. 1 and 2, respectively.

The monomers were initially reacted in a polar aprotic solvent (DMSO) at 165 °C [38–41]. Water that was generated from the condensation reaction was removed from the system by a constant nitrogen flow. The ionomer solutions became viscous after ~2 h and the reactions were stopped after 3 or 5.5 h (longer reaction times would result in gelation). After precipitation and drying, the polymer was soluble in DMAc, and the solutions were used to cast amber and fingernail creasable thin films. The ionomer structure is shown in Fig. 3.

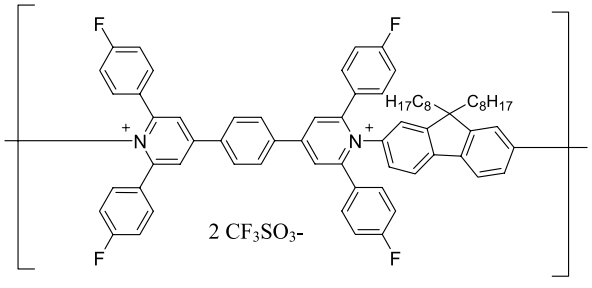

Fig. 3. Ionomer structure.

3.2. Preparation of IN nanocomposites

The SWNTs used in the IN nanocomposites were modified prior to use. As determined visually, the modified SWNTs were more readily wetted with DMAc than the as-received SWNTs. This allowed for shorter sonication times and better dispersion prior to the addition of any dispersing agent when using the s-tubes. The s-tubes/d-ionomer mixtures also appeared better dispersed by visual inspection than the neat tubes/d-ionomer mixtures. Three different methods were employed to further disperse the s-tubes in the ionomer. The first involved dispersing the s-tubes in DMAc via sonication, followed by incremental addition of ionomer. Upon initial addition and dissolution of the ionomer to the s-tube suspension, the mixture became homogenous and visually appeared to be a solution. Upon addition of more ionomer no visual agglomeration of the s-tubes was noticed and this method appeared to be a practical approach to disperse the s-tubes in the ionomer. However, at SWNT loading levels >1 wt%, significant amounts of solvent were required to initially disperse and sufficiently wet the s-tubes. In these instances if too little solvent was used, the initial sonication step would yield an extremely viscous mixture. The increased viscosity of the mixtures rendered the sonication virtually ineffective. However, if sufficient amounts of solvent were added to keep the viscosity low, the solution concentrations after complete ionomer addition were typically below 10% solids thus making film casting problematic.

A second method employed for the dispersion of the

Table 1
Composition of PIN films

Sample	CP2 wt%	Ionomer wt%	s-tube wt%
PIN control	77	23	0
PIN1	76.3	22.9	0.8
PIN2	61.7	37.1	1.2
PIN3	51.8	46.6	1.6
IS-PIN control	97.5	2.5	0
IS-PIN1	96.6	2.4	1
IS-PIN1 neat	96.6	2.4	1

s-tubes in the ionomer was an in-situ polymerization approach where the ionomer was prepared in the presence of the s-tubes. Due to poor dispersion of the s-tubes in DMSO prior to polymerization, DMAc was determined to be a better solvent for the polymerization and film casting. The nanocomposite films prepared by this method had some macroscopic agglomeration of SWNTs present at loading levels above 1 wt%. This was presumably due to some agglomeration of the s-tubes that occurred at the higher temperatures used for the polymerization.

A third method used to prepare IN films involved all of the same conditions described above for the in-situ approach except that films were not cast directly from the resulting solutions. The solutions were instead poured into water to isolate the material resulting in black tinted powders, which were washed with water and dried. The water in each case was clear and colorless after removal of the powder. Sonication and stirring in DMAc were effective at dispersing most of the s-tube agglomerates formed during the polymerization. Thin films were cast on warmed plates and immediately dried in a flowing air oven to preserve the dispersion obtained in the wet mixture. This was done to prevent reagglomeration of the s-tubes which tended to occur at the lower polymer concentrations mixtures ($<12\%$ solids) that these films were cast from. The reagglomeration was presumably due to higher rates of diffusion of the s-tubes in these lower solution viscosity mixtures. Thin films from these mixtures were fingernail creasable and depending on s-tube loading level, had little to no visual SWNT agglomeration. The 1 wt% film was visibly transparent, while the 2 and 3 wt% films had areas where the film was not transparent. The alternating transparent and non-transparent regions were very regular and created a patterned appearance on the surface.

3.3. Preparation of PIN nanocomposites

Nanocomposites were also prepared from polyimides, ionomer, and s-tubes by two different methods. The role of the ionomer in the simple mixing approach was to serve as a dispersing aid. After adding the ionomer dispersant, the homogeneous suspension was subsequently added to a solution of a soluble polyimide (LaRC™ CP2) while sonicating and stirring. The s-tubes initially agglomerated but upon stirring the mixtures became visually homogenous. However, visual s-tube agglomerates were present upon casting and drying films from these mixtures if there was not enough ionomer added. The PIN1 sample (Table 1) required a 30:1 ionomer:nanotube ratio to disperse the s-tubes well enough to provide a film with no visual agglomerates. This ionomer:nanotube ratio was used to prepare the rest of the PIN films. Using this mixing technique the PIN2 and PIN3 films were also prepared. These films were virtually transparent but the PIN2 film had a very light patterning on the film surface while the PIN3 film had more visual patterning on the film surface. When LaRC™ CP2 was dissolved in s-tube suspensions without the use of the dispersant visual agglomeration was noticed at much lower loading levels (approximately 0.13 wt%) [37].

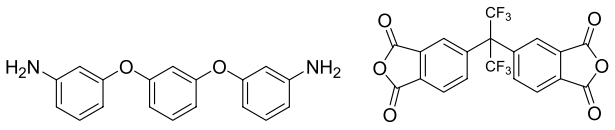

Fig. 4. LaRC™ CP2 monomers.

Although the use of the d-ionomer as a dispersant for the s-tubes in the polyimide was an effective way to make nanocomposites, a more desirable approach would be to use as little d-ionomer as possible so as not to affect the base properties of LaRC™ CP2. Thus IS-PIN nanocomposites were prepared by the in-situ polymerization of LaRC™ CP2 in s-tube/d-ionomer/DMAc suspensions. LaRC™ CP2 monomers (APB and 6FDA, Fig. 4) were sequentially added to s-tube/d-ionomer/DMAc suspensions under sonication. While preparing the IS-PIN1 sample the s-tube suspension appeared visually homogenous after 2.5 times the amount of d-ionomer was added relative to the s-tubes. Upon adding the monomers for LaRC™ CP2 and subsequent polymerization the suspension remained homogenous. A film was prepared from this mixture and was dried until tack-free before curing. At the polymer concentration ($\sim 14\%$) used to prepare the IS-PIN1 film, the mixture was quite viscous, thus making it possible to dry at room temperature. After drying and heating to remove the solvent, the film was transparent. Thus, a 2.5:1 ionomer:s-tube ratio was deemed sufficient to prepare films with as much as 1 wt% loading of s-tubes when using the in-situ approach. A film prepared in a similar fashion using neat tubes (IS-PIN1 neat) exhibited a hazy appearance and was not completely transparent. This was perhaps due to the decreased dispersability of the neat tubes which in turn decreased the optical transparency.

A summary of the preparatory methods used to prepare the nanocomposite films is given below in Fig. 5 and a listing of the amounts of the components in the PIN and IS-PIN films is shown in Table 1.

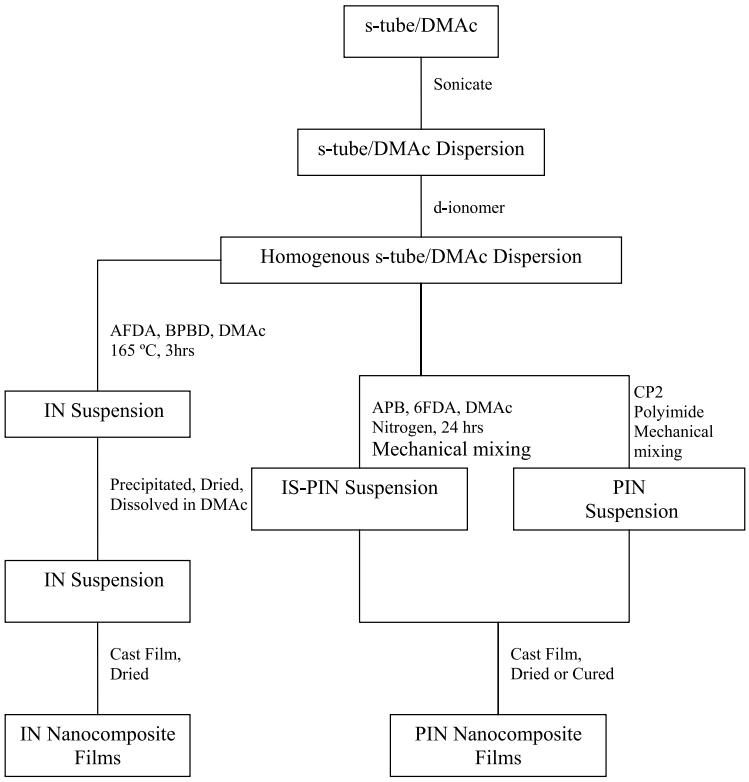

Fig. 5. Summary of nanocomposite preparation.

3.4. UV/Vis/NIR and Raman spectroscopy of nanocomposite films

The UV/Vis/NIR and Raman spectra for the ionomer based films are shown in Figs. 6 and 7, respectively. In both cases the spectra were not normalized for film thickness, thus the differences in intensities are not meaningful. The absorption peaks for the IN films in the 1000–1600 nm region are a distribution of transitions associated with the first pair of Van Hove singularities in the density of states of semiconducting HiPco SWNTs of various diameters. Those absorptions near 600 nm are attributed to the presence of metallic nanotubes in the sample [16,42]. The Raman spectrum for the as-received HiPco SWNTs and the spectrum of the s-tubes (Fig. 7) are nearly identical which indicates that the modification did not significantly alter the

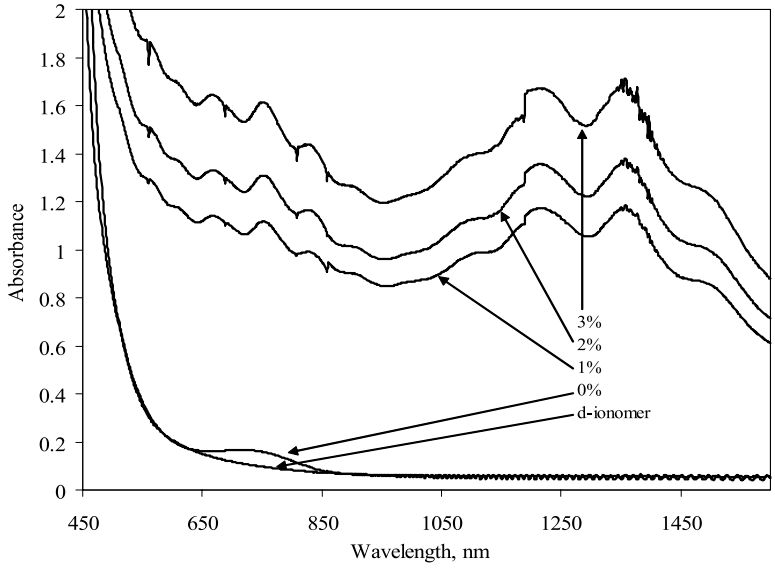

Fig. 6. UV/Vis/NIR spectra of IN films.

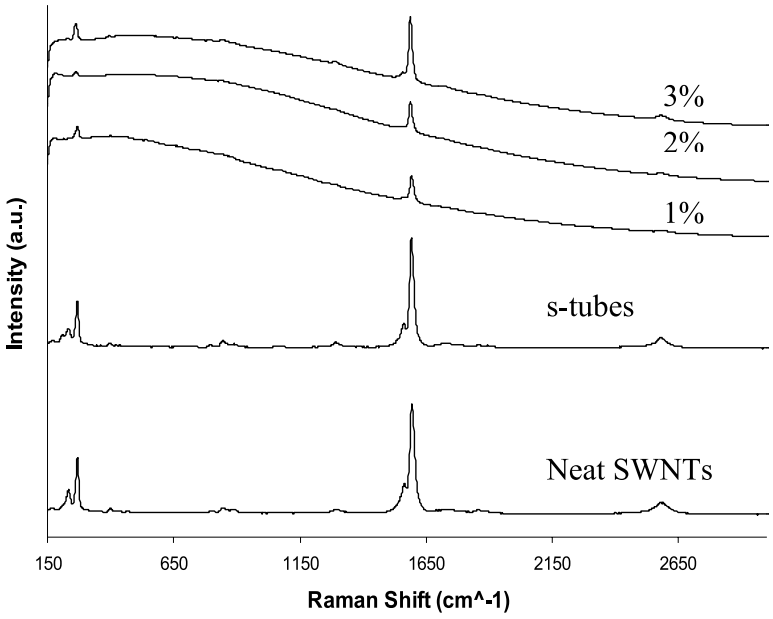

Fig. 7. Raman spectra of IN films.

structure of the SWNTs. The region of the Raman spectra near 270 cm^{-1}, which represents the radial breathing mode peaks, does not contain as many peaks in the nanocomposite films as in the s-tubes. This is similar to what was found in other polymer-SWNT nanocomposites [16]. The tangential mode ($\sim$1600 cm^{-1}) peaks which are found in the spectra of the s-tubes also occur in the spectra of the IN films indicating that the fundamental structure of the s-tubes was not significantly altered upon nanocomposite preparation [16].

The UV/Vis/NIR and Raman spectra for PIN films are shown in Figs. 8 and 9, respectively. The UV/Vis/NIR spectra of these films show the absorptions associated with semiconducting and metallic SWNTs and were comparable to those obtained for the IN nanocomposites. The control film (PIN control) was LaRC™ CP2 from SRS Technologies, Inc. containing the same amount of d-ionomer as the PIN1 film. The light yellow control film began to absorb at a lower wavelength than the amber d-ionomer film. The PIN1 film shows a major absorption at a similar wavelength and is light green in color. At higher levels of s-tubes the films are darker greenish-black colored. The Raman spectra of the PIN nanocomposites are similar to those of the IN nanocomposites and again show that the s-tubes were not significantly altered upon nanocomposite preparation.

The IS-PIN nanocomposite films and a control film were also characterized by UV/Vis/NIR and Raman spectroscopy. The spectra of these films are shown in Figs. 10 and 11. The data in the UV/Vis/NIR associated with the nanotubes are similar to that for the other films. However, as

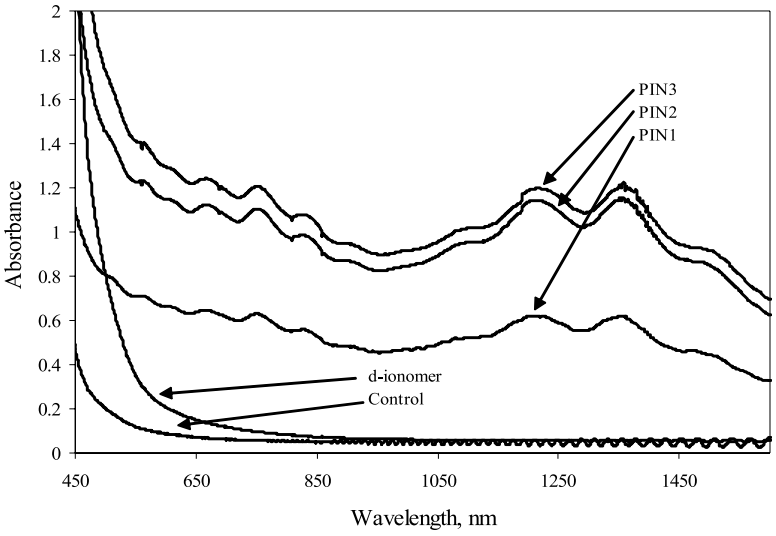

Fig. 8. UV/Vis/NIR spectra of PIN films.

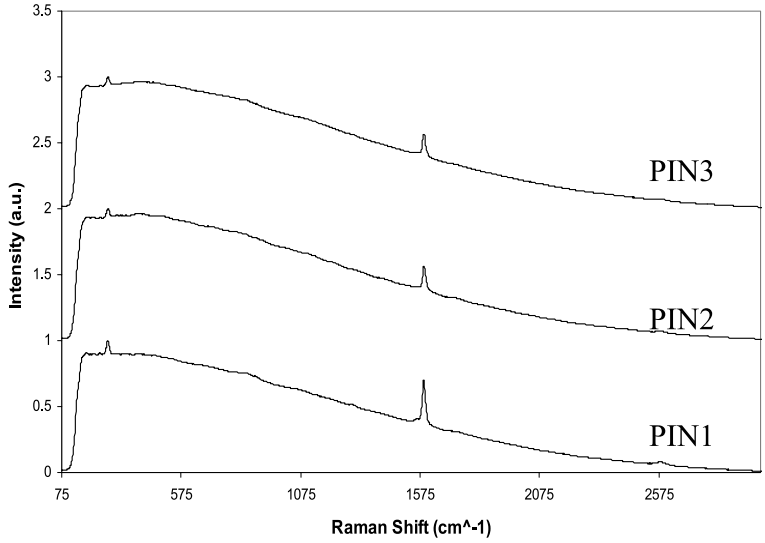

Fig. 9. Raman spectra of PIN films.

Table 2
Resistivity of IN films

s-tube loading (wt%)	Surface resistivity (Ω/square)	Volume resistivity (Ω cm)
0	$>10^{12}$	$>10^{12}$
1	5×10^{6}	9.3×10^{6}
2	6×10^{6}	7.5×10^{6}
3	4.7×10^{6}	5.1×10^{6}

indicated by the spectrum as well as visual inspection, IS-PIN1 films were highly colored (black). The difference in color between the IS-PIN1 films (black) and the PIN1 film (green) can be attributed to the lower amount of d-ionomer used in the in-situ film and perhaps better dispersion of the s-tubes in the PIN1 film as a result of the larger amount of ionomer. The IS-PIN control film had the same amount of d-ionomer as the IS-PIN1 film and was light yellow. The Raman spectrum of the IS-PIN films showed that the neat tubes and the s-tubes' structures were virtually unchanged during nanocomposite preparation.

3.5. Conductivity of nanocomposite films

The surface and volume resistivities were obtained for the nanocomposite films. Resistivity values obtained for the IN films were shown to be dependent upon the preparative method. For example, a 1 wt% IN film prepared by dissolving the ionomer in an s-tube/DMAc solution had surface resistivity of 10^{9} Ω/square, whereas a 1 wt% IN film prepared by the in-situ polymerization of the ionomer followed by casting a film from this mixture had a surface resistivity of 10^{5} Ω/square. This same solution prepared by

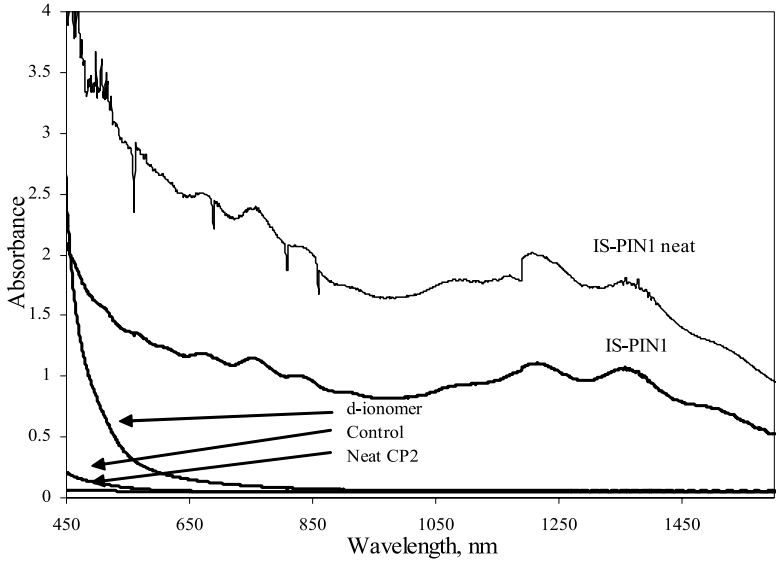

Fig. 10. UV/Vis/NIR spectra of IS-PIN films.

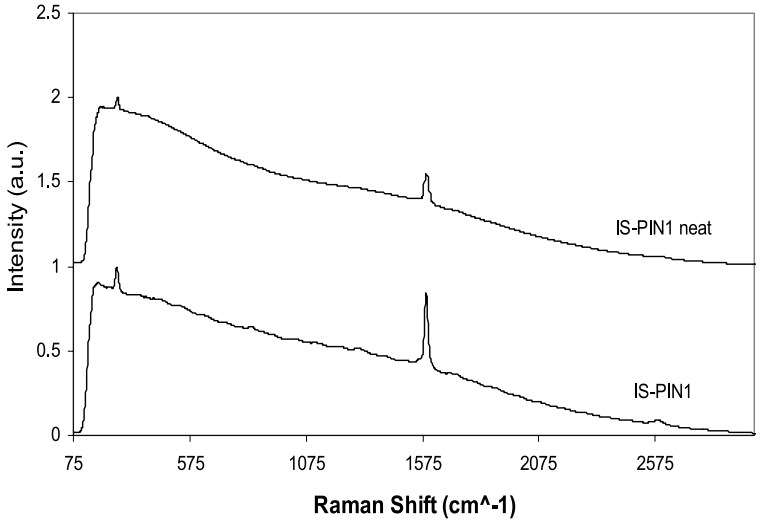

Fig. 11. Raman spectrum of IS-PIN films.

the in-situ approach was precipitated, redissolved in DMAc, and cast into a film had a surface resistivity of 10^6 Ω/square. These results suggest that different preparatory methods affect the s-tube dispersion and, therefore, the measured resistivity.

The resistivities of the IN films prepared via in-situ polymerization followed by precipitation, isolation and subsequent casting from DMAc are reported in Table 2. The introduction of s-tubes at 1 wt% significantly reduced the surface and volume resistivity of the films. However, increasing the concentration of the s-tubes above 1 wt% resulted in no further lowering of the resistivity of the hybrid films. Similar behavior was seen in other polyimide-SWNT films above the percolation threshold [16]. The conductivity may reach a plateau because of limitations due to the ratio of isomers (metallic:semiconducting) present in the s-tubes and/or a poorer distribution of the s-tubes is obtained at higher s-tube loadings.

The surface resistivities of the PIN films were higher than those obtained for the IN films (Table 3). The higher resistivity values may be attributed to either the difference in the resistivity of the polymers, or differences in s-tube distribution in the films. Although unexplained and contrary to the trend observed in the IN films, variations in the surface resistivities of the PIN films with s-tube loading were noted. The values for volume resistivity were also higher than the values obtained for the IN films. Excluding the control film, which was not conductive, the volume resistivities of the PIN films did not change as a function of d-ionomer loading or s-tube loading.

The resistivity values obtained for the IS-PIN1 films as well as two control films are shown below (Table 4). The surface and volume resistivities of the IS-PIN1 films are lower than the resistivity of the PIN1 film. One possible explanation is that the s-tubes are better distributed for improved conductivity when prepared via the in-situ method. The resistivity values for the films prepared with either the s-tubes or the neat tubes were similar although the volume resistivity was slightly higher in the sample prepared with the neat tubes. This implies that the electrical properties of the s-tubes were not damaged as a result of modification and the modification enhanced dispersion.

3.6. Tensile properties of nanocomposite films

Room temperature tensile properties of the nanocomposite films were obtained and compared with control samples. The properties for the IN films are reported in Table 5. An increase in mechanical properties, particularly modulus, was anticipated with the inclusion of the s-tubes, but little to no improvement in the tensile properties as a function of s-tube loading was observed. Recent report suggests that randomly dispersed SWNTs exist as a network structure of aggregated tubes and consequently did not provide the anticipated increase in modulus [16,43]. Conversely, if the SWNTs are aligned

Table 3
Resistivity of PIN films

Sample	Surface resistivity (Ω/square)	Volume resistivity (Ω cm)
PIN control	$>10^{12}$	$>10^{12}$
PIN1	2.8×10^{8}	3.8×10^{8}
PIN2	4.9×10^{7}	1.2×10^{8}
PIN3	1.1×10^{9}	3.0×10^{8}

Table 4
Resistivity of IS-PIN films

Film	Surface resistivity (Ω/square)	Volume resistivity (Ω cm)
LaRC™ CP2	$>10^{12}$	$>10^{12}$
IS-PIN control	$>10^{12}$	$>10^{12}$
IS-PIN1	9×10^{5}	3.8×10^{6}
IS-PIN1 neat	1.3×10^{5}	2.7×10^{7}

Table 5
Room temperature thin film tensile properties of IN films

s-tube Loading (wt%)	Modulus (GPa)	Strength (MPa)	Elongation (%)
0	3.1±0.1	69±7	4±1.0
1	3.0±0.1	69±3	6±0.9
2	2.8±0.1	55±6	3±0.8
3	3.0±0.1	55±3	3±0.4

the modulus can be increased [44]. The lowered strength and elongations in the 2 and 3% IN films, which were fingernail creasable, may be due to larger s-tube agglomerates (see Fig. 12) behaving as point defects in the films.

Table 6
Room temperature thin film tensile properties of PIN films

Sample	Modulus (GPa)	Strength (MPa)	Elongation (%)
Neat LaRC™ CP2	3.6±0.2	117±7	7±0.8
d-Ionomer	2.9±0.1	55±13	2±1.0
PIN control	3.2±0.1	103±9	5±0.7
PIN1	3.3±0.1	96±10	5±1.1
PIN2	3.4±0.1	89±2	4±0.2
PIN3	3.3±0.1	89±2	4±0.4

The mechanical properties of the PIN films as well as the control films were determined with the data presented in Table 6. As previously observed with the IN films, no

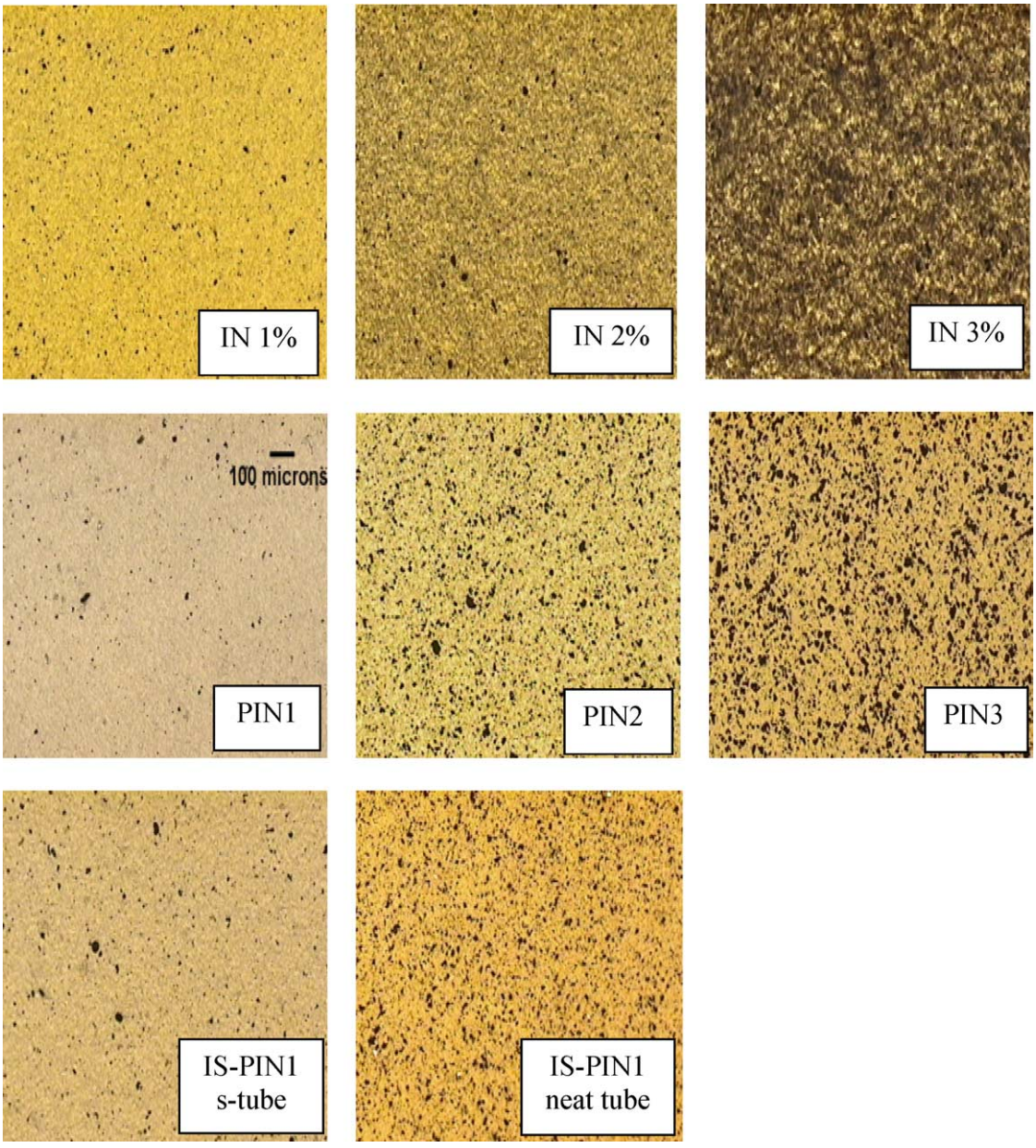

Fig. 12. Optical micrographs of nanocomposite films [IN Films (top row), PIN films (middle row), IS-PIN films (bottom row)] (scale in middle row is applicable to all the optical micrographs).

Table 7
Room temperature thin film tensile properties for IS-PIN films

Sample	Modulus (GPa)	Strength (MPa)	Elongation (%)
LaRC™ CP2	3.5±0.1	117±3	6±1.3
IS-PIN control	3.4±0.1	110±6	6±1.1
IS-PIN1	3.5±0.1	110±1	5±0.2
IS-PIN1 neat	3.5±0.1	118±1	6±0.3

significant increase in the tensile properties of the films occurred upon s-tube loading. The PIN control film had the exact same ratio of d-ionomer and polyimide as the PIN1 film and the values for modulus, strength, and elongation of these two films were similar. The control film also had a lower modulus, strength, and % elongation than neat LaRC™ CP2. This was expected since the d-ionomer film has lower tensile properties than the LaRC™ CP2. Since the ionomer lowers the tensile properties of the polymer mixtures, it was anticipated that the PIN2 and PIN3 films, which contain more ionomer, would exhibit some tensile property increases associated with the introduction of the s-tubes. However, no significant increase in mechanical properties was observed.

The tensile properties for the IS-PIN films (Table 7) showed that the properties of the control film were not significantly affected when compared to neat LaRC™ CP2 (prepared in-house). This is in contrast to the data obtained for the control film for the PIN films (Table 6), and was due to the lower amount of ionomer added in the IS-PIN control film. As previously observed, the inclusion of significant amounts of s-tube did not enhance the mechanical properties of the nanocomposite materials. This was the case when either the s-tubes or the neat tubes were used. The similarity in tensile properties between the two SWNT containing films suggests that there was no alteration of the mechanical properties of the s-tubes upon modification.

3.7. Optical and SEM images of nanocomposite films

The nanocomposites that were characterized for electrical and mechanical properties were also examined by microscopic methods. To examine the s-tube dispersion over a relatively large area of the films, optical micrographs were obtained. The optical micrographs shown in Fig. 12 were taken at 50× magnification. Two distinguishable features were present in all the micrographs. One of the features appeared as fine lines that were slightly darker than

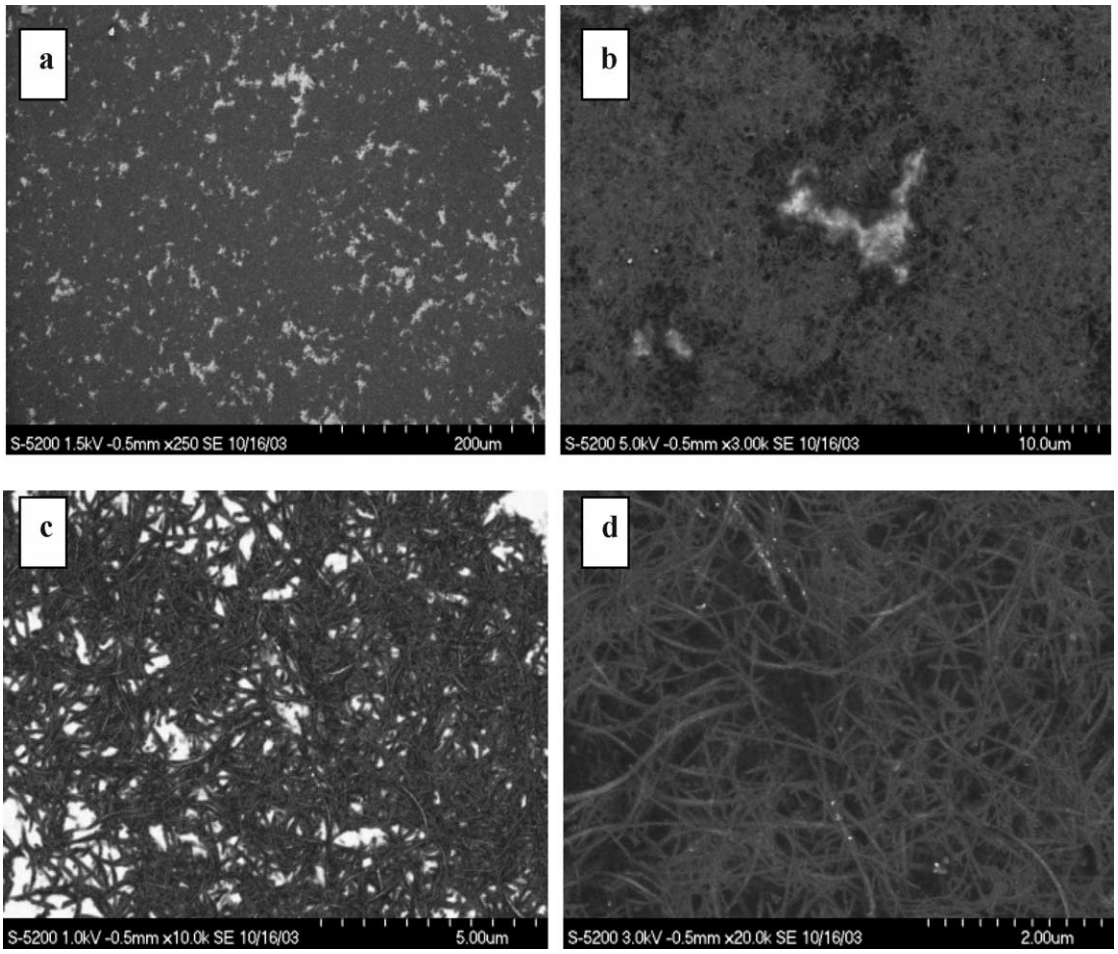

Fig. 13. HRSEM images of 3 wt% IN film [(a) 1.5 kV, 250× (b) 5.0 kV, 3000× (c) 1.0 kV, 10,000× (d) 3 kV, 20,000×].

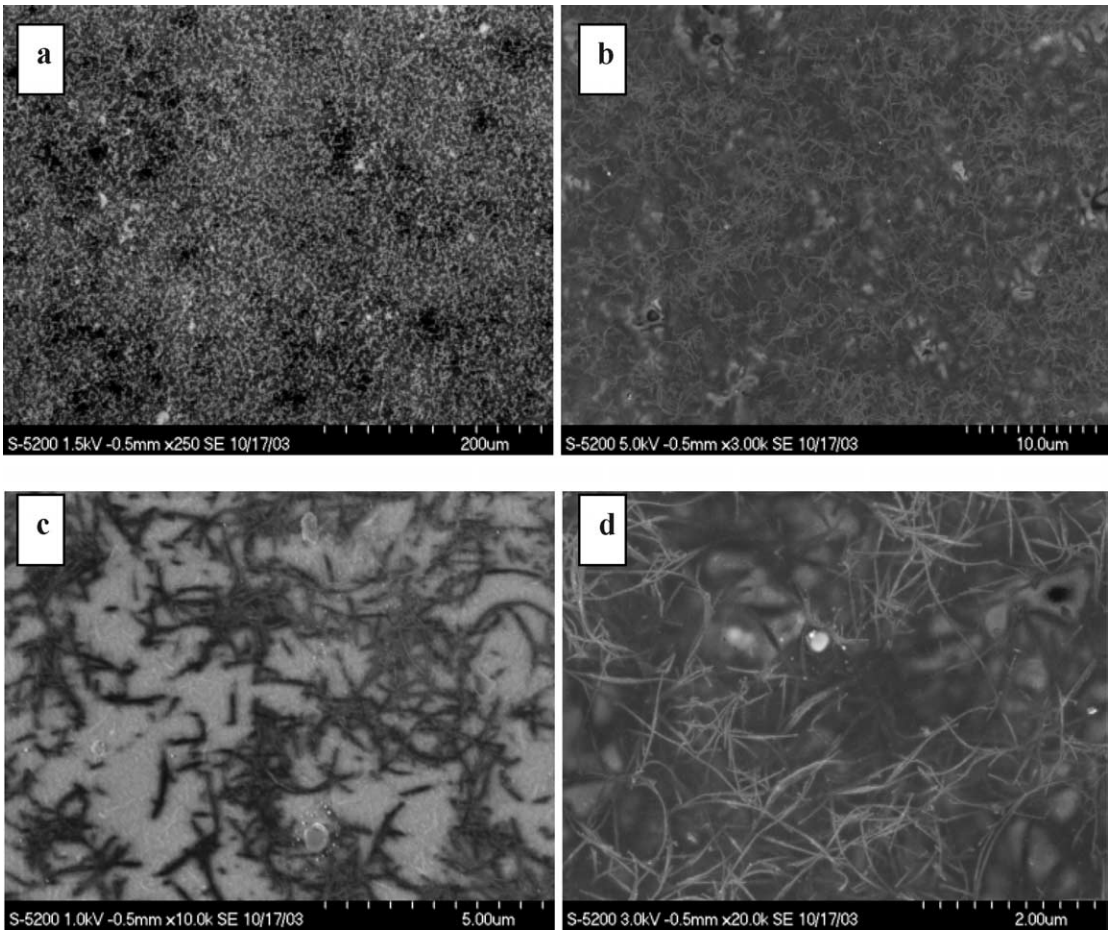

Fig. 14. HRSEM images of PIN1 films [(a) 1.5 kV, 250× (b) 5.0 kV, 3000× (c) 1.0 kV, 10,000× (d) 3 kV, 20,000×].

the background, while the other feature appears as black specks. These are suggested to represent networks of s-tubes and s-tube agglomerates, respectively. The network of s-tubes in all the micrographs appear uniformly distributed over the observed area. In the 2 and 3 wt% IN films (top row) the s-tube network was very noticeable, while the s-tube networks in the PIN2 and PIN3 films (middle row) were more difficult to see. Conversely, more agglomerates were present in the PIN2 and PIN3 films than in comparable IN films. The network in the IS-PIN1 film (s-tubes) appeared similar to the PIN1 film, but more agglomerates were noticeable. For all the films, it was noticed that higher concentration of ionomer reduced the amount of agglomerates. The IS-PIN1 neat film had more agglomerates than the similarly prepared film with s-tubes indicating that the s-tubes were better dispersed.

To further examine the dispersion of the s-tubes in the nanocomposite films, HRSEM images were collected. The HRSEM images were taken while the film surface was oriented normal to the beam. The contrast between the s-tubes and the polymer is due to variations in the beam-induced electric field and allows for a direct assessment of the dispersion of the SWNTs in polymer matrices [16,34]. In the IN films (Fig. 13) the s-tubes appeared to be uniformly dispersed in completely random arrays of rope-like networks. Lower magnification images of the IN films (Fig. 13(a and b)) give an assessment of the overall dispersion and showed some minor areas of polymer islands (bright regions) where no SWNTs were present. Overall the s-tubes appeared uniformly distributed throughout the entire polymer. In Fig. 13(b) the accelerating voltage was increased to produce a contrast reversal to directly visualize the s-tubes. The same methods were used to examine the film at higher magnifications (Fig. 13(c and d)). Polymer islands were visible as bright regions in Fig. 13(c) at low voltage and the s-tubes were visible under the higher applied accelerating voltage in Fig. 13(d). The s-tubes appeared well dispersed throughout the thickness of the film. The sizes of the s-tubes are difficult to assign with the HRSEM as the nanotubes will always appear larger than actual size. With this in mind the HRSEM images most likely represent small bundles of SWNTs on the order of tens of nanometers.

In general the images shown for the specimens indicate good dispersion of the s-tubes at relatively high weight loadings. The ionomer may work well as a dispersing agent because it is attracted to the π character of the tube surface. The aromatic portion of the ionomer is assumed to be associated with the surface of the nanotubes as a result of

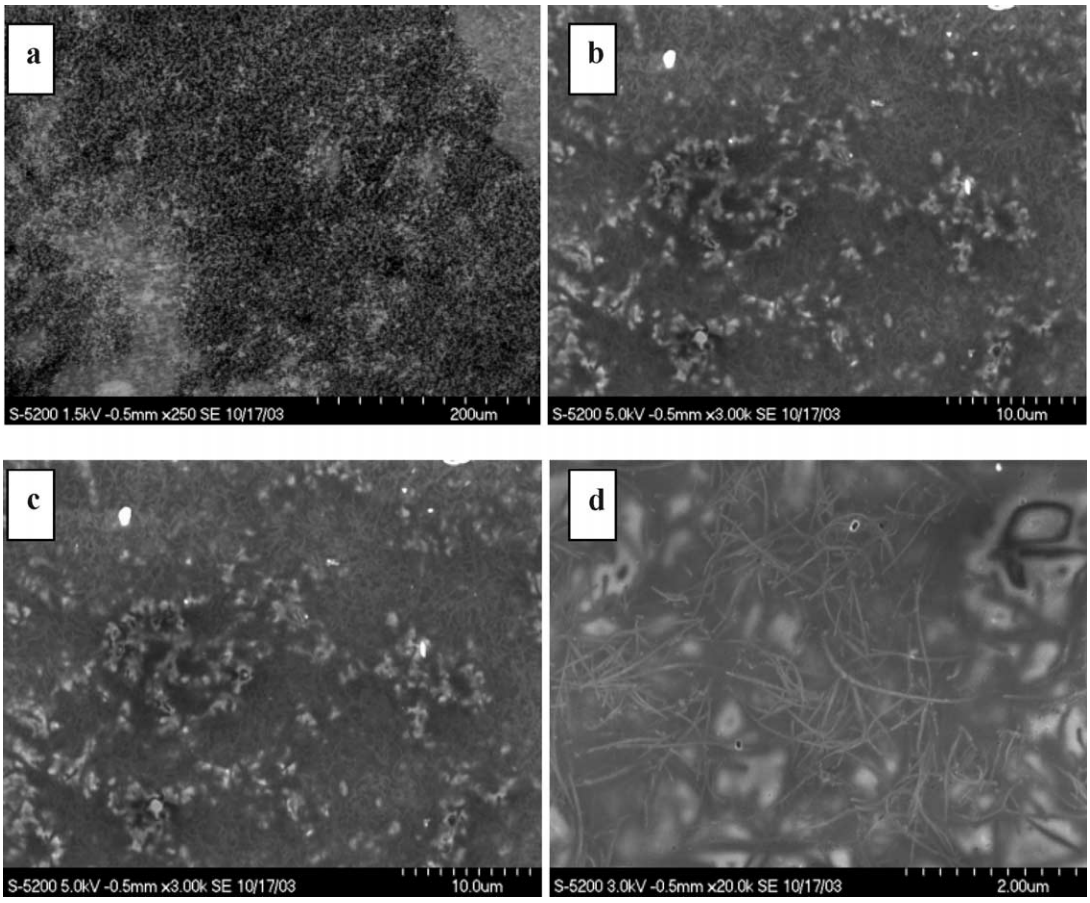

Fig. 15. HRSEM images of IS-PIN1 film (s-tube) [(a) 1.5 kV, 250× (b) 5.0 kV, 3000× (c) 1.0 kV, 10,000× (d) 3 kV, 20,000×].

orbital overlap, while the alkyl portions are assumed to orient away from the nanotube surface. [1]. Possibilities for enhanced SWNT dispersion include: 1) the ionomer is tightly wrapping the s-tubes as is suggested for other conjugated polymers [21–29,31,32] 2) the polymer is anchored to the surface in local regions [19] affording a much looser wrap or 3) multiple polymer chains are wrapping or anchoring on the same nanotube [23].

HRSEM images in Fig. 14 show similar results for the PIN1 film as were seen for the IN films. In all of the images the s-tubes appeared well dispersed and exhibited a random rope-like structure. In Fig. 14(a) the low magnification image shows that the s-tubes were well distributed throughout the entire polymer. Upon going to higher accelerating voltages the s- tubes were directly visualized as in Fig. 14(b and d). This indicates a robust network of small s-tube bundles is present throughout the film as clearly seen in Fig. 14(d).

Although low magnification HRSEM of the IS-PIN1 film (s-tube) (Fig. 15(a)) shows that the s-tubes were uniformly dispersed on the surface of the film, images taken with higher accelerating voltages reveal areas of high polymer content. However, Fig. 15(b and d) still show an extensive network of small s-tube bundles throughout the film. Similar statements can be made about the IS-PIN1 neat film containing neat tubes (Fig. 16), however, it appeared that the bundle size is slightly larger.

The HRSEM images indicate that the SWNTs are randomly oriented throughout the polymer in each of the samples. This finding helps to explain the absence of major changes in the mechanical data [16,43]. However, neither the optical micrographs nor the HRSEM images can be used to explain the differences in electrical properties from sample to sample.

4. Summary

Nanocomposites containing SWNTs and an aromatic ionomer were prepared using three different methods and the resulting films characterized for electrical and mechanical properties as well as SWNT dispersion. Nanocomposites containing SWNTs and ionomer were conductive upon addition of SWNTs at 1, 2, and 3%, but the mechanical properties were not significantly affected even at these high loading levels. As much as 1 wt% SWNTs could be incorporated into polyimides when the ionomer was used to aid in dispersion. The polyimide films were also rendered conductive, but the mechanical properties were not improved. The in-situ preparation of the polyimide in the

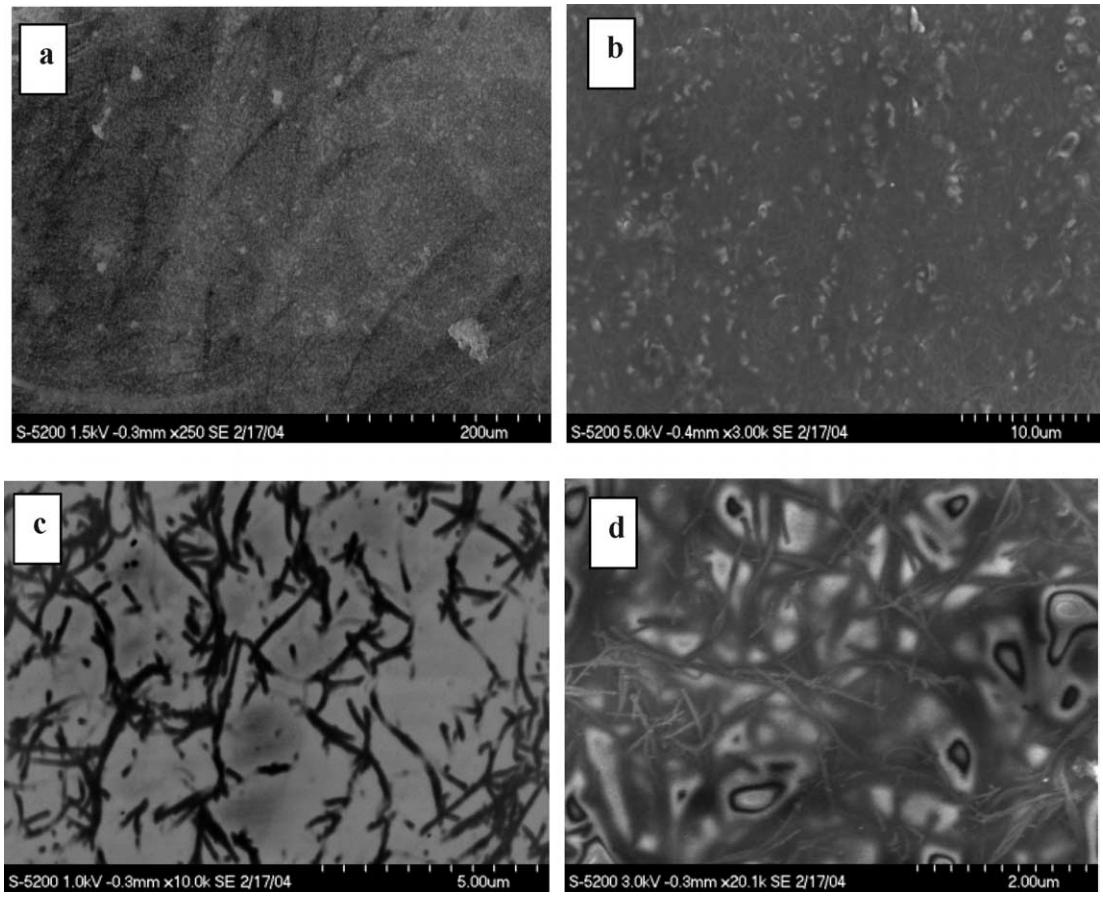

Fig. 16. HRSEM images of IS-PIN1 film (neat tube) [(a) 1.5 kV, 250× (b) 5.0 kV, 3000× (c) 1.0 kV, 10,000× (d) 3 kV, 20,000×].

presence of pre-dispersed SWNTs appeared to be the best way to prepare polyimide-SWNT nanocomposites. A ratio of 2.5:1 was deemed sufficient to disperse up to 1 wt% s-tube in LaRC™ CP2 using this method. A similarly prepared film that contained neat tubes exhibited similar electrical and mechanical properties but the neat tubes did not disperse as well as the s-tubes. However, in all the nanocomposites the use of the ionomer did aid in SWNT dispersion which could be useful in the preparation of other polymer-SWNT nanocomposites.

References

[1] Lin T, Bajpai V, Ji T, Dai L. Aust J Chem 2003;56:635.
[2] Watson KA, Smith Jr. JG, Connell JW. Society for the Advancement of Materials and Process Engineering Technical Conference Series 2001;33:1551.
[3] Smith Jr. JG, Watson KA, Thompson CM, Connell JW. Society for the Advancement of Materials and Process Engineering Technical Conference Series 2002;34:365.
[4] Smith JG Jr., Connell JW, Lillehei P, Watson KA, Thompson CM. Materials Research SocietySpring 2002 Session T, On-line Proceedings, 2002;733E:T3.5. www.mrs.org/publications/epubs/proceedings/spring2002/t/.
[5] Park C, Ounaies Z, Watson KA, Crooks RE, Smith Jr. JG, Lowther SE, et al. Chem Phys Lett 2002;364:303.
[6] Mukhopadhyay K, Dwivedi CD, Mathur GN. Carbon 2002;40:1373.
[7] Chen J, Hamon MA, Hu H, Chen Y, Rao AM, Eklund PC, et al. Science 1998;282:95.
[8] Niyogi S, Hamon MA, Hu H, Zhao B, Bhowmik P, Sen R, et al. Acc Chem Res 2002;35:1105.
[9] Sun Y-P, Fu K, Lin Y, Huang W. Acc Chem Res 2002;35:1096.
[10] Hill DE, Lin Y, Rao AM, Allard LF, Sun Y-P. Macromolecules 2002;35:9466.
[11] Aizawa M, Shaffer MSP. Chem Phys Lett 2003;368:121.
[12] Banerjee S, Wong SS. JACS 2002;124:8940.
[13] Bahr JL, Tour JM. Chem Mater 2001;13:3823.
[14] Dyke CA, Tour JM. JACS 2003;125:1156.
[15] Holzinger M, Abraham J, Whelan P, Graupner R, Ley L, Henrich F, et al. JACS 2003;125:8566.
[16] Smith Jr. JG, Connell JW, Delozier DM, Lillehei PT, Watson KA, Lin Y, et al. Polymer 2004;45:825.
[17] Islam MF, Rojas E, Bergey DM, Johnson AT, Yodh AG. Nano Lett 2002;3:269.
[18] Star A, Liu Y, Gant K, Ridvan L, Stoddart JF, Steuerman DW, et al. Macromolecules 2003;36:553.
[19] Chen RJ, Zhang Y, Wang D, Dai H. JACS 2001;123:3838.
[20] Star A, Steuerman DW, Heath JR, Stoddart JF. Angew Chem Int Ed 2002;41:2508.
[21] Hirsch A. Angew Chem Int Ed 2002;41:1853.
[22] Ago H, Shaffer MSP, Ginger DS, Windle AH, Friend RH. Phys Rev B: Condens Mat Mater Phys 2000;61:2286.
[23] O'Connell MJ, Boul P, Ericson LM, Huffman C, Wang Y, Haroz E, et al. Chem Phys Lett 2001;342:265.
[24] Curran S, Ajayan PM, Blau WJ, Carroll DL, Coleman JN, Dalton AB, et al. Adv Mater 1998;10:1091.

[25 Coleman JN, Dalton AB, Curran S, Rubio A, Davey AP, Drury A, et al. Adv Mater 2000;12:213.
[26 Curran S, Davey AP, Coleman JN, Dalton AB, McCarthy B, Maier S, et al. Synth Met 1999;103:2559.
[27 McCarthy B, Coleman JN, Czerw R, Dalton AB, Carroll DL, Blau WJ. Synth Met 2001;121:1225.
[28] Dalton AB, Stephan C, Coleman JN, McCarthy B, Ajayan PM, Lefrant S, et al. J Phys Chem B 2000;104:10012.
[29] Steuerman DW, Star A, Narizzano R, Choi H, Ries RS, Nicolini C, et al. J Phys Chem B 2002;106:3124.
[30] Wise KE, Park C, Siochi EJ, Harrison JS. Chem Phys Lett 2004;391:207.
[31] Star A, Stoddart JF, Steuerman DW, Diehl M, Boukai A, Wong EW, et al. Angew Chem Int Ed 2001;40:1721.
[32] Xu H, Tang BZ. Polym Mater Sci Eng 1999;80:408.
[33] Wang J, Musameh M, Lin Y. JACS 2003;125:2408.
[34] Landi BJ, Raffaelle RP, Heben MJ, Alleman JL, VanDerveer W, Gennett T. Nano Lett 2002;2:1329.
[35] Fukushima T, Kosaka A, Ishimura Y, Yamamoto T, Takigawa T, Ishii N, et al. Science 2003;300:2072.
[36] Ranger M, Rondeau D, Leclerc M. Macromolecules 1997;30:7686.
[37] Delozier DM, Connell JW, Smith JG Jr., Watson KA. 'Preparation and Characterization of Space Durable Polymer Nanocomposite Films from Functionalized Carbon Nanotubes', 3rd World Congress Nanocomposites 2003, November 10–12; 2003.
[38] Harris FW, Chuang KC, Huang SA, Janimak JJ, Cheng SZD. Polymer 1994;23:4940.
[39] Tigelaar DM, Klein DJ, Xu TB, Su J, Bryant RB. In press, High Performance Polymer.
[40] Lin F, Cheng SZD, Harris FW. Polymer 2002;43:3421.
[41] Huang SAX, Chuang KC, Cheng SZD, Harris FW. Polymer 2000;41: 5001.
[42] Chiang IW, Brinson BE, Huang AY, Willis PA, Bronikowski M, Margrave JL, et al. J Phys Chem B 2001;105:8297.
[43] Shaefer DW, Zhao J, Brown JM, Anderson DP, Tomlin DW. Chem Phys Lett 2003;375:369.
[44] Siochi EJ, Working DC, Park C, Lillehei PT, Rouse JH, Topping CC, et al. Composites: Part B 2004;35:439.